The Journal of Experimental Biology 206, 2241-2255

doi:10.1242/jeb.00430

Functional characterization of a glutamate/aspartate transporter from the mosquito *Aedes aegypti*

Anita Umesh[1,2,*], Bruce N. Cohen[3], Linda S. Ross[2] and Sarjeet S. Gill[1,2,†]

[1]*Environmental Toxicology Graduate Program*, [2]*Department of Cell Biology and Neuroscience, University of California, Riverside, Riverside, CA 92521, USA* and [3]*Division of Biology, California Institute of Technology, Pasadena, CA 91125, USA*

*Present address: Division of Pulmonary and Critical Care Medicine, Johns Hopkins University School of Medicine, Baltimore, MD 21224, USA

†Author for correspondence (e-mail: sarjeet.gill@ucr.edu)

Accepted 3 April 2003

Summary

Glutamate elicits a variety of effects in insects, including inhibitory and excitatory signals at both neuromuscular junctions and brain. Insect glutamatergic neurotransmission has been studied in great depth especially from the standpoint of the receptor-mediated effects, but the molecular mechanisms involved in the termination of the numerous glutamatergic signals have only recently begun to receive attention. In vertebrates, glutamatergic signals are terminated by Na^+/K^+-dependent high-affinity excitatory amino acid transporters (EAAT), which have been cloned and characterized extensively. Cloning and characterization of a few insect homologues have followed, but functional information for these homologues is still limited. Here we report a study conducted on a cloned mosquito EAAT homologue isolated from the vector of the dengue virus, *Aedes aegypti*. The deduced amino acid sequence of the protein, AeaEAAT, exhibits 40–50% identity with mammalian EAATs, and 45–50% identity to other insect EAATs characterized thus far. It transports L-glutamate as well as L- and D-aspartate with high affinity in the micromolar range, and demonstrates a substrate-elicited anion conductance when heterologously expressed in *Xenopus laevis* oocytes, as found with mammalian homologues. Analysis of the spatial distribution of the protein demonstrates high expression levels in the adult thorax, which is mostly observed in the thoracic ganglia. Together, the work presented here provides a thorough examination of the role played by glutamate transport in *Ae. aegypti*.

Key words: glutamate/aspartate transporter, mosquito, *Aedes aegypti*, neurotransmitter, amino acid, electrophysiology, localization.

Introduction

Glutamate is a well-established neurotransmitter in both vertebrates and invertebrates. In mammals it is the principal excitatory transmitter in the central nervous system, although excess extracellular glutamate concentrations are associated with various neurological states including ischemia, amyotropic lateral sclerosis and Alzheimer's disease, and must therefore be tightly regulated (Maragakis and Rothstein, 2001). In contrast to vertebrates, glutamate primarily acts as an excitatory transmitter at the neuromuscular junction in invertebrates, analogous to the role played by acetylcholine in vertebrate neuromuscular junctions (Kerkut et al., 1965; Usherwood, 1967; Usherwood and Machili, 1966). The action of glutamate in insects is further complicated by its additional ability to elicit inhibitory responses at insect muscles, as well as mixed excitatory and inhibitory responses in the central nervous system (Burrows, 1996; Cull-Candy, 1976; Darlison, 1992; Homberg, 1994; Sattelle, 1992).

In mammals, it is believed that Na^+- and K^+-dependent high-affinity transport systems are responsible for regulating extracellular glutamate levels as well as terminating glutamatergic signals in the central nervous system (for a review, see Danbolt, 2001). Five transporters with the ability to transport L-glutamate and L-and D-aspartate have been identified in humans. They have been designated EAAT (Excitatory Amino Acid Transporter) 1–5, having 50–60% amino acid identity with each other (Seal and Amara, 1999). These proteins drive the uphill transport of glutamate by dissipating the electrochemical Na^+ gradient generated by Na^+/K^+-ATPase. It is currently accepted in mammals that glutamate transport occurs with the cotransport of $3Na^+$ and $1H^+$, and a countertransport of $1K^+$ with every molecule of glutamate (Levy et al., 1998; Zerangue and Kavanaugh, 1996b). Additionally, glutamate evokes an anion channel activity intrinsic to the EAATs: a property which, however, is not directly coupled to substrate translocation (Fairman et al., 1995; Wadiche et al., 1995a).

In insects, early biochemical studies have shown the existence of Na^+-dependent L-glutamate transport systems in both muscle and central nervous systems. Examples include Na^+-dependent glutamate transport on isolated abdominal nerve cords from adult *Periplaneta americana*, as well as autoradiographic transport studies in the excitatory neuromuscular junctions of locust localizing Na^+-dependent glutamate transport to nerve endings and surrounding glia (Evans, 1975; van Marle et al., 1983).

The availability of cDNA sequences encoding mammalian EAATs, coupled with the advent of molecular cloning, has allowed for the cloning and isolation of EAAT homologues from a number of insect species within the last 5 years. In particular, insect EAAT homologues have been cloned by independent groups from the brain and embryo of *Drosophila melanogaster* (dEAAT1 and dEAAT2) as well as the brains of caterpillar *Trichoplusia ni* (TrnEAAT), cockroach *Diploptera punctata* (DipEAAT) and honeybee *Apis mellifera* (AmEAAT) (Besson et al., 1999; Donly et al., 1997, 2000; Kawano et al., 1999; Kucharski et al., 2000; Seal et al., 1998). With the exception of AmEAAT, all insect homologues cloned thus far have been heterologously expressed and functionally characterized as Na^+-dependent high-affinity glutamate and aspartate transporters with affinity in the micromolar range (Besson et al., 1999, 2000; Donly et al., 1997, 2000; Kawano et al., 1999; Kucharski et al., 2000; Seal et al., 1998). Electrophysiological studies on dEAAT1 have illustrated a substrate-elicited anion conductance that is stoichiometrically uncoupled from substrate translocation, much like the mammalian EAATs (Fairman et al., 1995; Seal et al., 1998; Wadiche et al., 1995b). Amongst such similarities, however, certain differences have been noted, such as a preference for L- and D-aspartate as substrates over L-glutamate for dEAAT2; a preference for L-asparatate over D-aspartate by DipEAAT; and abolished substrate transport by dEAAT1 in the absence of both intracellular and extracellular chloride (Besson et al., 2000; Donly et al., 2000; Seal et al., 1998).

Attempts at elucidating the spatial localization of the insect EAATs at the mRNA level for dEAAT1, dEAAT2 and AmEAAT, have demonstrated almost exclusive localization to parts of the brain insect brain (Besson et al., 1999; Seal et al., 1998; Soustelle et al., 2002). A recent immunohistochemical study on TrnEAAT, however, demonstrated expression in larval skeletal muscle fibers (Gardiner et al., 2002).

In spite of the fact that glutamate performs a plethora of roles in insects, and that a number of insect transporters for glutamate have been characterized, information available for the termination of insect glutamatergic signals is still relatively sparse. In light of this, we present a comprehensive study on a glutamate and aspartate transporter from the mosquito *Aedes aegypti* (AeaEAAT), which encompasses cloning and characterization from pharmacological, electrophysiological, and spatial localization standpoints. *Ae. aegypti* is the major vector for the dengue virus; the work presented here therefore represents the first such kind from a blood-feeding insect. Given the recent completion of the *Anopheles gambiae* genome project, together with the historic interest in the biology of the mosquito as a vector for various human diseases, the work presented here is a timely contribution to the understanding of this disease vector.

Materials and methods

Maintenance of animals

Aedes aegypti L. were maintained in a light:dark photoperiod of 16 h:8 h, at 26°C and 77% relative humidity. Larvae were fed with a mixture of yeast and dry dog food (1:3 w/w) dissolved in water, adults were reared on sugar water and females were given weekly mouse blood meals.

Midgut/Malpighian tubule cDNA library construction

Poly(A)$^+$ RNA was isolated from isolated midgut and Malpighian tubules of adult female *Aedes aegypti*. The mRNA was then used for the construction of cDNA using a cDNA synthesis kit from (GIBCO BRL Life Technologies, Gaithersburg, MD, USA). The cDNA (approximately 1.5 μg) was separated by size-exclusion chromatography on a Superose 6 column using a SMART system (Pharmacia LKB Biotechnology, Piscataway, NJ, USA) as previously described (Mbungu et al., 1995). The >2kb cDNA was ligated to *Not*I/*Sal*I-cut, dephosphorylated pSport1 vector and electroporated into DH10B cells. The size of the unamplified library was 130 000 clones, 95% of which were recombinants. Isolation and analysis of individual cDNA clones demonstrated the presence of large inserts in this library.

Isolation of clone and construction in expression vector

The gene encoding AeaEAAT, initially named BC10, was identified during an EST project that randomly sequenced approximately 2000 different genes expressed in the cDNA library above. The open reading frame (ORF) was subcloned into the expression vector pBSAMV containing a T7 promoter, through the *Nco*I and *Fse*I restriction enzyme sites (Chiu et al., 2000). These restriction sites were engineered into the 5′ and 3′ ends of the ORF, respectively, by polymerase chain reaction (PCR) using primers containing the sites. The PCR product generated by Expand (Roche, Palo Alto, CA, USA) was gel purified, and initially ligated to pCR2.1 (Invitrogen, Carlsbad, CA, USA) according to the manufacturer's specifications. Clones putatively containing the desired product were sequenced to confirm the lack of any PCR-generated errors using ABI Prism cycle sequencing. The clone with the correct sequence was subsequently subcloned into the pBSAMV vector (Chiu et al., 2000), and will herein be referred to as pBSAMVBC10.

In vitro *transcription/translation*

The plasmid pBSAMVBC10 containing the AeaEAAT ORF was *in vitro* transcribed and translated using the TNT T7-Coupled Reticulocyte Lysate System (Promega, Madison, WI, USA). A sample (4 μl) of the total reaction was separated by

discontinuous 8% SDS-PAGE as described previously (Laemmli, 1970). The gel was stained with Coomassie Blue, destained, treated in Entensify enhancing solutions (Dupont-NEN, Boston, MA, USA), and dried before exposure to X-ray film for 3 days.

Transient transfections

HeLa cells were maintained in Minimum Essential Medium (Invitrogen, Carlsbad, CA, USA) containing 1.5 g $NaHCO_3$, sodium pyruvate (Invitrogen), non-essential amino acids (Invitrogen), penicillin/streptomycin (Invitrogen) and 10% fetal bovine serum (Summit Biotechnologies, Greeley, CO, USA) at 37°C and 5% CO_2. Transient transfections utilizing the T7/vaccinia virus method were generally carried out in 48-well plates using serum-free medium for all steps (Blakely et al., 1991). Briefly, $5–7\times10^4$ cells per well were plated the night before transfection in the above medium lacking antibiotics, of which 2 wells were counted on the day of the transfection to obtain an average number of cells per well. A virus multiplicity of infection of 5, 0.3 μl of lipofectin (Invitrogen), 1 μl PLUS reagent (Invitrogen), and 100 ng of DNA was used per well in all cases. Lipofectin was diluted in medium 30–35 min before mixing with DNA, which itself was preincubated with the PLUS reagent for 15 min beforehand. Cells were infected with virus (30 m, 37℃/5% CO_2) with shaking every 10 min, and the lipofectin/DNA/PLUS mixture was overlayed.

Transport assay in mammalian cells

Transport assays were carried out between 18 and 24 h after infection/transfection. Cells were washed once with PBS, and incubated for 15 min with uptake buffer (120 mmol l^{-1} NaCl, 4.7 mmol l^{-1} KCl, 10 mmol l^{-1} Hepes, pH 7.5, 5 mmol l^{-1} Tris-Cl, pH 7.4, 1.2 mmol l^{-1} KH_2PO_4, 2 mmol l^{-1} $CaCl_2$, 1.2 mmol l^{-1} $MgSO_4$) containing glucose before performing the transport assay in duplicate. In order to determine substrate specificity, cells were incubated with a mixture of cold substrate (100 μmol l^{-1}) and ^{3}H-labeled substrate (30 nmol l^{-1}; Amersham, Piscataway, NJ, USA) used as a tracer, initially for 10–20 min. The substrates that were transported (L-glutamate, L-aspartate and D-aspartate) were further analysed for ion dependence, time course and dose–response studies.

Time course, ion dependence and kinetic analyses

A time course study was performed on all three substrates, where the duration of transport was varied. Upon determining the time during which transport followed a linear time course, this time point (5 min) was used in all subsequent transport assays.

The dependence of substrate transport on the major extracellular ions was determined by substituting equimolar choline chloride for NaCl in the assay buffer, while two types of anions, gluconate and acetate, were used in independent experiments to replace chloride ions.

Dose–response studies were performed to obtain the affinity and kinetic parameters (K_m and V_{max}), by varying the cold substrate concentration between 0.1 μmol l^{-1} and 500 μmol l^{-1} on a logarithmic scale. Experiments were performed in triplicate to obtain mean K_m and V_{max} values, calculated by a least-squares fit to the Michaelis–Menton equation and Eadie–Hofstee transformation using Origin 6.0 (Microcal, Northampton, MA, USA).

Pharmacology

Inhibition studies were carried out with 1 μmol l^{-1} cold substrate and 30 nmol l^{-1} ^{3}H-labeled substrate, so as to render the concentration of substrate negligible when mathematically determining the K_i, such that the IC_{50} approximates the K_i as described (Cheng and Prusoff, 1973a). A three-point screen of 3, 100 and 3000 μmol l^{-1} inhibitor concentration was used initially in order to eliminate compounds that essentially had no effect on transport. Others were consequently subjected to a further inhibition assay, where inhibitor concentrations were varied on a logarithmic scale, typically between 1 nmol l^{-1} and 3 mmol l^{-1}.

Electrophysiology

Heterologous expression in *Xenopus laevis* oocytes was utilized to study the electrophysiological properties of AeaEAAT *via* two-electrode voltage clamp (TEV-200, Dagan Instruments, Minneapolis, MN, USA) interfaced to an IBM-compatible PC using a Digidata 1200 A/D controlled using the pCLAMP 6.0 program suite (Axon Instruments, Foster City, CA, USA). The expression construct pBSAMVBC10 was cut with *Not*I for runoff *in vitro* transcription using the Ambion T7 mMessage mMachine kit (Ambion, Austin TX, USA). Stages V and VI *Xenopus* oocytes were prepared using standard protocols, injected with 35 ng of cRNA, and incubated for 3–6 days in ND96 (96 mmol l^{-1} NaCl, 2 mmol l^{-1} KCl, 1 mmol l^{-1} $CaCl_2$, 1 mmol l^{-1} $MgCl_2$, 5 mmol l^{-1} Hepes, pH 7.5) supplemented with gentamycin at 18°C before recordings. Current responses were acquired at room temperature and analyzed with either Clampfit 8.0 (Axon Instruments, Foster City, CA, USA) or ORIGIN 6.0 (MicroCal Software, Northampton, MA, USA). Signals were filtered with a 2 kHz low-pass filter and a 3 mol l^{-1} KCl agar bridge was used to reduce junction potentials. Microelectrodes were filled with filtered 3 mol l^{-1} KCl solution, with resistances of less than 1 MΩ for both current passing and recording electrodes. For the superfusing of saline solution, a Perkin–Elmer Model 410 liquid chromatography pump was used, supplying a continuous flow of ND-96 buffer at a flow rate of 1.0 ml min^{-1}. A Rheodyne injection valve was used to apply substrates for dose–response analysis in 170 μl volumes, providing a 5 s exposure of substrate to the oocyte. Concentration–response relationships to determine EC_{50} values were obtained from oocytes clamped at –60 mV by measuring the peak current amplitude as a function of substrate concentration. Results were normalized to current evoked by the highest substrate concentration used, and subsequently fit to the equation $I=I_{max}S/(EC_{50}+S)$, where I is the peak current amplitude, I_{max} is the peak current amplitude evoked by the highest substrate concentration, and S is the concentration of substrate.

In reversed-transport studies, oocytes clamped at –60 mV were exposed to a high potassium buffer containing 98 mmol l^{-1} KCl, 1 mmol l^{-1} $MgCl_2$, 1.8 mmol l^{-1} $CaCl_2$ and 5 mmol l^{-1} Hepes (pH 7.5).

Current–voltage relationships were determined either by measurement of steady-state currents in response to bath application of substrates or by off-line subtraction of control current records obtained during 1 ms voltage pulses to potentials between –60 and +50 mV from corresponding current records in the presence of substrate. Sodium substitution studies were carried out in saline containing equimolar choline chloride instead of NaCl. External chloride was replaced by either gluconate, nitrate or thiocyanate salts as indicated, at concentrations equivalent to the chloride salts used in ND96. Intracellular chloride depletion experiments were performed as described in Wadiche et al. (1995a), by placing oocytes in chloride-free buffer substituted with gluconate for at least 20 h prior to use.

Xenopus *oocyte transport assay*

Substrate-transport assays in *Xenopus* oocytes were performed by exposing oocytes to ^{3}H-radiolabeled substrate (30 nmol l^{-1} L-glutamate, L-aspartate and D-aspartate; Amersham) for 5 min at room temperature. Oocytes were then rapidly washed three times in ice-cold buffer in order to prevent any possibility of reversed transport, upon which they were lysed in 10% SDS and subjected to scintillation counting.

For cases in which transport assays were performed under two-electrode voltage clamp, oocytes were clamped at –60 mV and exposed to radioactive ligand for 5 s, then washed for 10 s with the respective saline, and subsequently lysed and counted for accumulated radioactivity as described above.

Antibody production and purification

A synthetic peptide of 15 amino acids, corresponding to the C-terminal 14 amino acids of AeaEAAT, plus a cysteine at the N terminus of these 14 residues (CPSSEINGKTQRNSL) was synthesized (MGIF, University of Georgia). The peptide was conjugated to a maleimide-activated form of keyhole limpet hemocyanin (KLH; Pierce, Rockford, IL, USA) according to the manufacturer's instructions, immunized in rabbits and affinity-purified essentially as described (Umesh and Gill, 2002).

Preparation of membranes from Ae. aegypti

Membranes were isolated from adult *Ae. aegypti* using a differential centrifugation protocol. Head, thorax and abdomen were separated from male and female *Ae. aegypti* anesthetized in CO_2. Briefly, tissues were suspended in ice-cold Tris-HCl buffer (50 mmol l^{-1}, pH 7.4) containing phenylmethylsulfonyl fluoride (PMSF; 1 mmol l^{-1}) and protease cocktail inhibitor (Roche Diagnostics, Indianapolis, IN, USA), homogenized with 30 strokes using a Dounce homogenizer, and centrifuged (3000 ***g***, 4°C, 10 min). The post-nuclear supernatant was centrifuged (10 000 ***g***, 4°C, 10 min) to remove mitochondria, and the resulting supernatant was further centrifuged to pellet the membranes (100 000 ***g***, 1 h, 4°C) using a Beckman Ti 42.2 rotor. Final pellets were resuspended in the homogenization buffer, upon which protein concentrations were determined with the BCA Protein Assay Kit (Pierce).

Preparation of membranes from X. laevis *oocytes*

Membranes were prepared from *Xenopus* oocytes injected with cRNA of pBSAMVBC10 and that of a *D. melanogaster* sodium channel, of which the latter served as a negative control (Buller and White, 1992). Briefly, oocytes were homogenized in Buffer A (150 mmol l^{-1} NaCl, 10 mmol l^{-1} magnesium acetate, 20 mmol l^{-1} Tris-Cl, 0.1 mmol l^{-1} PMSF, pH 7.6) containing sucrose (10% w/v) at a concentration of 25 oocytes ml^{-1} of buffer. Homogenates were overlayed on a discontinuous sucrose gradient consisting of 20% and 50% sucrose, and subsequently centrifuged (15 000 ***g***, 30 min, 4°C). The layer visible at the interface of 20% and 50% sucrose, representing the membrane portion, was carefully removed, diluted in 5 volumes of buffer A and recovered by centrifugation (100 000 ***g***, 1.5 h, 4°C).

SDS-PAGE and western analysis

Membranes and cytosol of *Ae. aegypti*, as well as *X. laevis* oocyte membranes, were analyzed by SDS-PAGE and western blotting. Protein samples were treated with Laemmli sample buffer (37°C, 30 min). Subsequently, samples were separated by an 8% polyacrylamide gel at a concentration of 25 and 9 μg per lane for the tissue samples and oocyte membranes, respectively. For western analysis, samples separated by SDS-PAGE were electrotransferred onto Immobilon P membranes (0.45 mm; Millipore, Billerica, MA, USA) using a tank transfer system (80 V, 3 h, 4°C). Upon blocking (1 h, room temperature) with 3% BSA in PBS containing 0.05% Tween-20 (PBST), membranes were incubated with affinity-purified AeaEAAT antibody (1 μg, overnight, 4°C) diluted in PBST containing 1% BSA. As a negative control, membranes with identical samples were incubated with primary antibody that had been preadsorbed with peptide (10 μmol l^{-1}). Upon washing in PBST, membranes were incubated with horseradish peroxidase (HRP)-coupled donkey anti-rabbit IgG (Amersham) diluted 1:3000 in 1% BSA/PBST (1 h, room temperature), washed extensively, and proteins were ultimately detected using enhanced chemiluminescence (Amersham).

Immunohistochemistry

Immunohistochemical studies were performed on adult thorax. Upon separation of the thorax and fixation in alcoholic Bouin's solution (overnight, 4°C), tissues were sectioned after paraffin embedding as described before (Umesh and Gill, 2002). Sections were blocked in PBS-Triton X-100 (0.2%) (PBS-Tx, pH 7.4) containing normal goat serum (NGS, 1%) and BSA (0.1%) for 30 min, and then incubated with the α-AeaEAAT (1/200 dilution in blocker, 4°C, overnight). After extensive washes with PBS-Tx, sections were incubated with HRP-labeled goat anti rabbit IgG (American Qualex, San

Clemente, CA, USA) diluted 1/1000 in blocker, washed thoroughly with PBS-Tx and stained using 3-amino 9-ethylcarbazol as a substrate (Umesh and Gill, 2002). Slides were visualized with a Zeiss Axiovert microscope (Carl Zeiss, Thornwood, NY, USA). All images were ultimately imported into Adobe Photoshop (version 6.0, Adobe, Sunnyvale, CA, USA) in which they were assembled and labeled.

Results

Isolation and sequence analysis of AeaEAAT from Aedes aegypti

Clones were isolated from a cDNA library prepared from the midgut and Malpighian tubule tissues of *Ae. aegypti*, and sequenced by ABI cycle sequencing. Of the clones isolated and sequenced one, designated BC10, showed sequence homology to the known EAATs. Its open reading frame of 1443 base pairs (bp) encoded a protein of 481 amino acids (aa), designated AeaEAAT (*Ae. aegypti* excitatory aa transporter; GenBank Accession number AY249244). At the aa level, AeaEAAT was 40–50% identical to other known EAATs, with highest identity to known insect EAATs, having 55.3, 51.5 and 48.2% identity to DipEAAT, dEAAT1 and TrnEAAT, respectively. Fig. 1A shows an alignment generated by ClustalW, representing AeaEAAT sequence similarity with insect EAATs that have been functionally characterized to date. As for known EAATs, hydropathy analysis of AeaEAAT gave six strongly hydrophobic domains in the N-terminal half of the protein, corresponding to distinct regions of transmembrane domains (overlined in Fig. 1A). The C-terminal half, having the highest degree of sequence conservation, gave one large domain of hydrophobicity. The

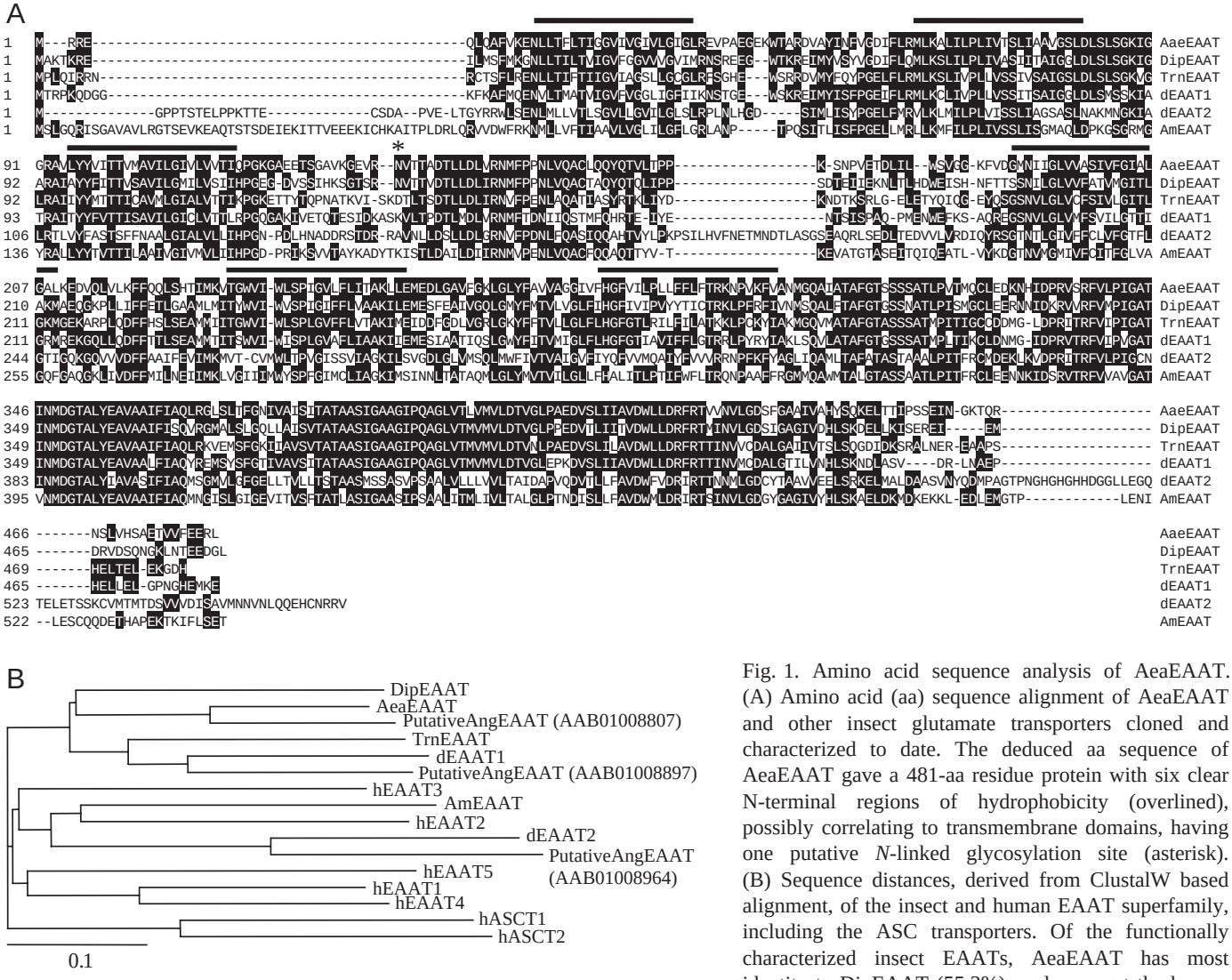

Fig. 1. Amino acid sequence analysis of AeaEAAT. (A) Amino acid (aa) sequence alignment of AeaEAAT and other insect glutamate transporters cloned and characterized to date. The deduced aa sequence of AeaEAAT gave a 481-aa residue protein with six clear N-terminal regions of hydrophobicity (overlined), possibly correlating to transmembrane domains, having one putative *N*-linked glycosylation site (asterisk). (B) Sequence distances, derived from ClustalW based alignment, of the insect and human EAAT superfamily, including the ASC transporters. Of the functionally characterized insect EAATs, AeaEAAT has most identity to DipEAAT (55.3%), and amongst the human counterparts has highest identity to hEAAT3 (47%). Included are putative EAATs from the completed genome of *Anopheles gambiae* (GenBank accession numbers: AAB01008807; AAB01008797, AAB01008964), the first of which has 74.9% identity to AeaEAAT. AeaEAAT, *Aedes aegypti*; AmEAAT, *Apis mellifera*; DipEAAT, *Diploptera punctata*; dEAAT1 and dEAAT2, *Drosophila melanogaster*; TrnEAAT, *Trichoplusia ni*; hEAAT1-5, human; hASCT, human alanine serine cysteine transporter.

deduced amino acid sequence of AeaEAAT additionally gave one putative *N*-linked glycosylation site between transmembrane domains 2 and 3 (asterisk in Fig. 1A).

The dendrogram analysis (Fig. 1B) includes members of the human EAAT superfamily consisting of hEAAT1-5 and related system ASC transporters, ASCT1 and ASCT2, which transport alanine, serine, threonine and cysteine. Also included are cloned insect EAATs and homologous sequences from the completed genome of *Anopheles gambiae*. Amongst the five subtypes of mammalian EAATs identified thus far, the above mentioned insect transporters collectively are most identical to hEAAT3, with 47.7% identity to AeaEAAT. The completed genomic sequence of *An. gambiae* gave three sequences representing putative members of the EAAT family: AAB01008807, AAB01008797 and AAB01008964, with the deduced amino acid sequences yielding proteins with 75.1, 52.0 and 33.5% identity to AeaEAAT, respectively.

Heterologous expression of AeaEAAT

The AeaEAAT open reading frame was subcloned into the expression vector pBSAMV, whose expression is driven by the T7 promoter. *In vitro* transcription and translation of this subclone gave a protein migrating at 42 kDa when separated by SDS-PAGE (Fig. 2, lane 1).

Heterologous expression of pBSAMVBC10 in both HeLa (Fig. 3) and CV-1 (data not shown) cells showed transport of substrates typical for this family of proteins, namely, L-glutamate, and L- and D-aspartic acid. Negative controls were initially conducted using the same vector containing a different transporter, MasIne (Chiu et al., 2000), but showed no difference from transfections conducted without DNA (data not shown).

Transport was Na^+-dependent, as replacement of Na^+ ions in the assay buffer with choline reduced uptake to background levels (Fig. 3A). On the other hand, transport was independent of Cl^-, since replacement with each of two types of anions, acetate and gluconate, made no significant difference (Fig. 3B).

AeaEAAT is a high-affinity transporter of its substrates, having K_m values of approximately 30 and 10 μmol l^{-1} for L-glutamate and the two types of aspartate, respectively (Table 1). In all three cases transport was saturable, with the dose–response relationship following Michaelis–Menten kinetics. Similar affinity parameters were observed when AeaEAAT was independently expressed in both HeLa and CV-1 cells (data not shown). The V_{max} values were determined to be 6.0, 3.0 and 6.9 fmol $cell^{-1}$ h^{-1} for L-glutamate, L-aspartate and D-aspartate, respectively. From these values, the efficacy (V_{max}/K_m) of transport by AeaEAAT was highest for D-aspartate (0.6), being double that of L-aspartate (0.3), and triple that of L-glutamate (0.2). Substrate transport was not inhibited

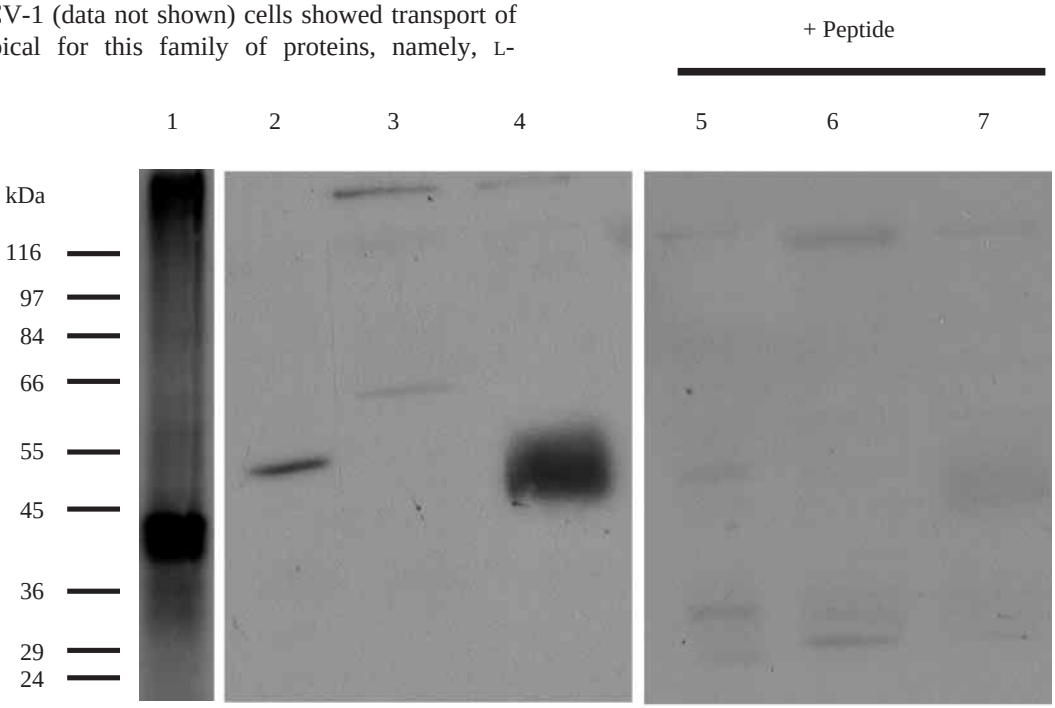

Fig. 2. *In vitro* transcription/translation of AeaEAAT and western analysis. *In vitro* transcription and translation of the AeaEAAT cDNA produces a translation product that migrates at approximately 40 kDa on an 8% SDS-PAGE gel (lane 1). AeaEAAT is expressed in both the head of the adult *Ae. aegypti* (lane 2), as well as in *Xenopus laevis* oocytes injected with the cRNA encoding AeaEAAT as a protein (lane 4) with mobility of 55 kDa. Membranes prepared from the whole head of adult *Ae. aegypti* and from *Xenopus laevis* oocytes expressing AeaEAAT were separated by 8% SDS-PAGE, transferred to Immobilon P (Millipore), and subjected to western analysis, using the affinity-purified α-AeaEAT antibody. Preincubation of the primary antibody with the antigenic peptide abolished any signal. Lanes 2 and 5, adult *Ae. aegypti* head membranes; lanes 3 and 6, *Xenopus laevis* oocytes injected with cRNA of a *Drosophila* sodium channel; lanes 4 and 7, *X. laevis* oocytes injected with cRNA of pBSAMVBC10. Note that lanes 5–7 are probed with the primary antibody upon preadsorption with the antigenic peptide. The positions of molecular mass (kDa) proteins are shown.

by D-glutamate (Table 2), indicating that for glutamate, AeaEAAT demonstrates stereoselective transport of the L-congener.

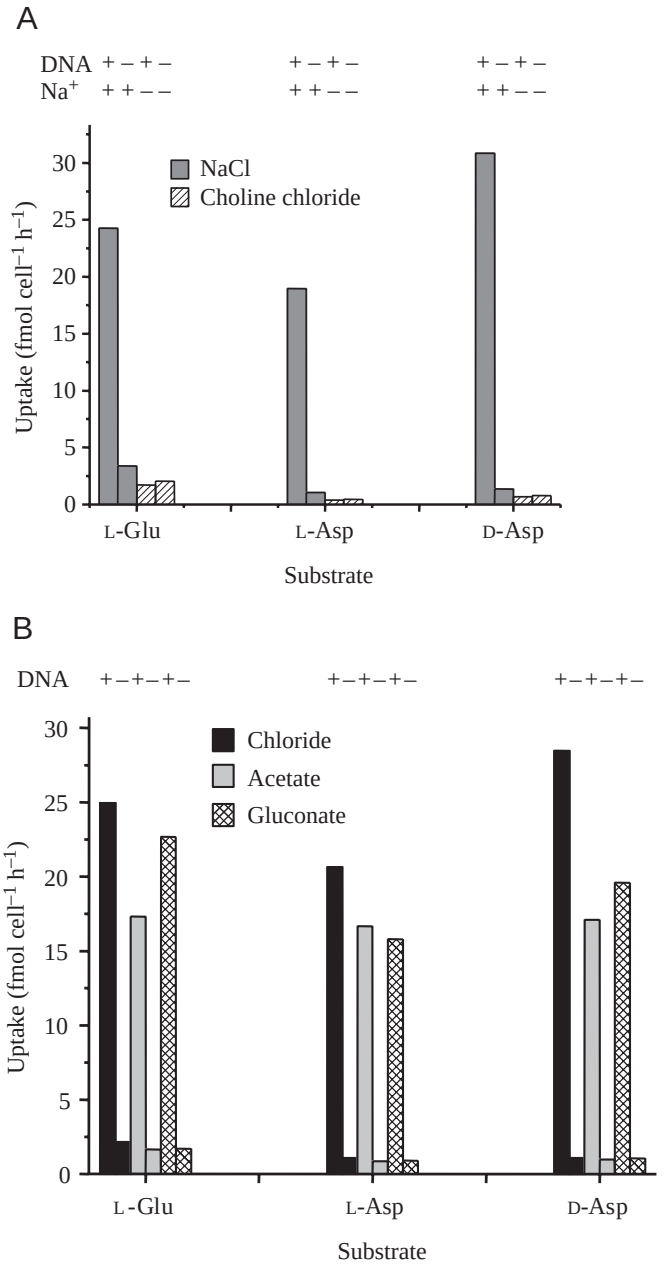

Fig. 3. Ion dependence of substrate transport. HeLa cells were transfected either with pBSAMVBC10 carrying the open reading frame of AeaEAAT or with no DNA (–, control), and were assayed for the transport of its substrates, L-glutamate, L-aspartate and D-aspartate, 24 h post infection/transfection. Both A and B are the result of one representative experiment, which was repeated three times and shown to give the same result qualitatively each time. (A) Sodium dependence of substrate transport was assessed by substituting equimolar choline chloride for NaCl in the transport assay buffer (striped bars). (B) Anion dependence of substrate transport was determined by replacing chloride ions in the transport assay buffer either with equimolar concentrations of acetate (gray bars) or gluconate (hatched bars).

We tested the ability of the 20 amino acids to compete with transport of D-aspartate (Fig. 4), the non-metabolizable substrate, at a competitor concentration of 5 mmol l^{-1}. As expected, the earlier determined high-affinity substrates (i.e. L-glutamate and L-aspartate) most strongly competed D-aspartate transport. In addition, we found that L-cysteine inhibited D-aspartate uptake to 12% of control levels, and that L-asparagine and L-glutamine also inhibited the substrate transport by 27.5% and 70% of control levels, respectively. At the concentrations used, inhibition by these amino acids was statistically significant at the 99% confidence interval.

Pharmacology

In an initial screen, various compounds in amounts of 3, 100 and 3000 μmol l^{-1} were tested for their ability to independently block the AeaEAAT-mediated transport of L-glutamate and D-aspartate. 30 nmol l^{-1} ^{3}H-labeled and 100 μmol l^{-1} unlabeled substrate were used in the initial screen. Of the compounds tested, *N*-methyl-D-aspartate and kainic acid had no effect on transport, even at 3 mmol l^{-1} (Table 2). Thereafter, the amount of substrate used was reduced to a total of 1 μmol l^{-1}, so as to approximate the IC_{50} to K_i (Cheng and Prusoff, 1973b). The IC_{50} (equivalent to the calculated K_i) values of 11 compounds, DL-*threo*-benzoxyaspartic acid (DL-TBOA), *trans*-pyrrolidine-2,4-dicarboxylate (t-PDC), L-aspartate-β-hydroxymate, DL-*threo*-β-hydroxyaspartic acid (TBHA), L-cysteine, L-cysteic acid, serine-*O*-sulfate, L-cysteine sulfinic acid, α-amino adipic acid, β-glutamate and D-glutamate were determined by using

Table 1. *Kinetics of substrate transport for excitatory amino acid transporters (EAATs)*

	K_m (μmol l^{-1})		
Protein	L-Glutamate	L-Aspartate	D-Aspartate
AeaEAAT	29.4±4.6	10.1±0.9	13.3±3.0
dEAAT1[a]	72±3	31±4	92±9
dEAAT2[b]	184.9±12.4	33.7±6.2	29.2±6.1
TrnEAAT	39.4±3.1		20.4
DipEAAT	30.5±4.7		222.4
hEAAT1[c]	48±10		60±12
hEAAT2[c]	97±4		54±9
hEAAT3[c]	62±8		47±9

[a]Seal et al. (1998) expression in COS-7 cells.
[b]Besson et al. (2000) expression in S2 cells.
[c]Arriza et al. (1994) expression in COS-7 cells.

Aea, *Aedes aegypti*; d, *Drosophila melanogaster*; Trn, *Trichoplusia ni*; Dip, *Diploptera punctata*; h, human.

HeLa cells infected with vTF7-3 recombinant vaccinia virus and transfected with pBSAMVBC10 were assayed for transport of 30 nmol l^{-1} ^{3}H-labeled and varying concentrations (0–500 μmol l^{-1}) of unlabeled substrate for 5 min.

Affinity (K_m) values shown are means ± S.E.M. of 3–4 individual experiments and are compared to published values from orthologues.

Corresponding V_{max} values were 6.0, 3.0 and 6.9 fmol $cell^{-1}$ h^{-1} for L-Glu, L-Asp and D-Asp, respectively.

Table 2. *Inhibition of substrate transport*

	K_i (μmol l^{-1})				
Inhibitor	AeaEAT	TrnEAT[1]	EAAT1[2]	EAAT2[2]	EAAT3[2]
DL-TBOA	23.7±2.1		42[3]	5.7[3]	6
tPDC	91±19	110±15.3	79±7	8±2	61±14
TBHA	9.2±2.9	32.4±4.8	32±8	19±6	25±5
SOS	29±5	88.9±21.8	107±8	1157±275	150±52
CA	6.6±3.3	18.4±4.4	10±3	10±2	19±9
CSA	7.1±3		14±7	6±1	17±2
L-Cys	336				
LAβH	97.5±13.7	316±52	369±70	184±27	133±34
α-AA	524±55				
β-Glu	651±20		297±118	156±37	307±48
D-Glu	1060±70				
L-Asn	2670±210				
KA	>3000		>3000	59±18	>3000
NMDA	>3000				

DL-TBOA, DL-threo-benzoxyaspartic acid; tPDC, *trans*-pyrrolidine dicarboxylic acid; TBHA, beta hydroxyaspartate; SOS, serine-o-sulfate; CA, cysteic acid; CSA, cysteine sulfinic acid; L-cys, L-cysteine; LAβH, L-aspartate-β-hydroxymate; α-AA, α-amino adipic acid; β-Glu, β-glutamate; D-Glu, D-glutamate; L-Asn, L-asparagine; KA, kainic acid; NMDA, *N*-methyl-D-aspartate.

[1]Donly et al. (1997).

[2]Arriza et al. (1994).

[3]Shimamoto et al. (1998).

AeaEAAT-expressing HeLa cells were exposed to 1 μmol l^{-1} cold and 30 nmol l^{-1} ^{3}H-labeled D-aspartate in the presence of logarithmically varying concentrations of known glutamate transport inhibitors. Transport was terminated after 5 min, and the K_i values determined from IC_{50} values as described previously (Cheng and Prusoff, 1973).

Values are compared to those published for TrnEAAT and hEAAT1–3 (see Table 1 for abbreviations).

logarithmically increasing concentrations of the various inhibitors. Overall, the inhibitors were equally effective at inhibiting the transport of both D-aspartate (Table 2) and L-glutamate (data not shown). Of the compounds tested, those involved in the cysteine oxidation pathway such as L-cysteic acid and L-cysteine sulfinic acid, as well as TBHA, were the most effective inhibitors, with calculated K_i values of approximately 6.6±3.3, 7.1±3 and 9.2±2.9 μmol l^{-1}, respectively. The most notable difference in AeaEAAT pharmacology was inhibition by serine-*O*-sulfate, for which the K_i was 29 μmol l^{-1}. This compound was twice as potent at inhibiting transport by AeaEAAT than TrnEAAT, and three times as potent than hEAAT3. A universal inhibitor of all EAAT subtypes, t-PDC, blocked D-aspartate transport with a K_i of 91±19 μmol l^{-1}, and DL-TBOA, a non-substrate EAAT inhibitor, gave a K_i value of 23.7±2.1 μmol l^{-1}.

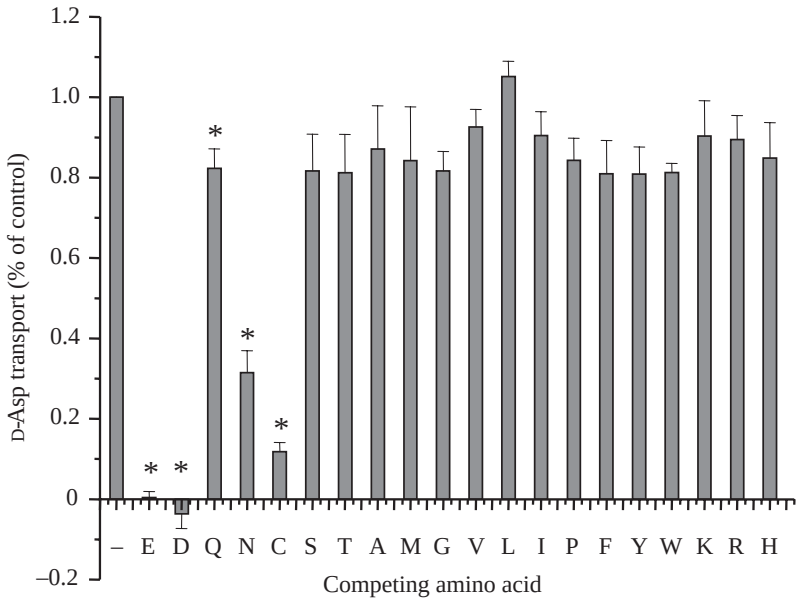

Fig. 4. Amino acid inhibition of D-aspartate transport. The ability of the 20 amino acids (each at 5 mmol l^{-1}) to compete the transport of D-aspartate (as a mixture of 1 μmol l^{-1} cold and 30 nmol l^{-1} ^{3}H-D-aspartate) was examined. Values are a mean of triplicate experiments, plotted as a percentage of D-aspartate transport (fmol cell^{-1} h^{-1}) in the absence of any competing amino acid. Asterisks indicate significant inhibition at the 99% confidence interval. Note that the results for tyrosine (Y) and tryptophan (W) also appeared to give significant inhibition, but are not indicated by asterisks due to the acidic conditions required for dissolving these amino acids at 5 mmol l^{-1}, which skewed the results. Amino acids are indicated by the single letter code. –, control (no competing amino acid).

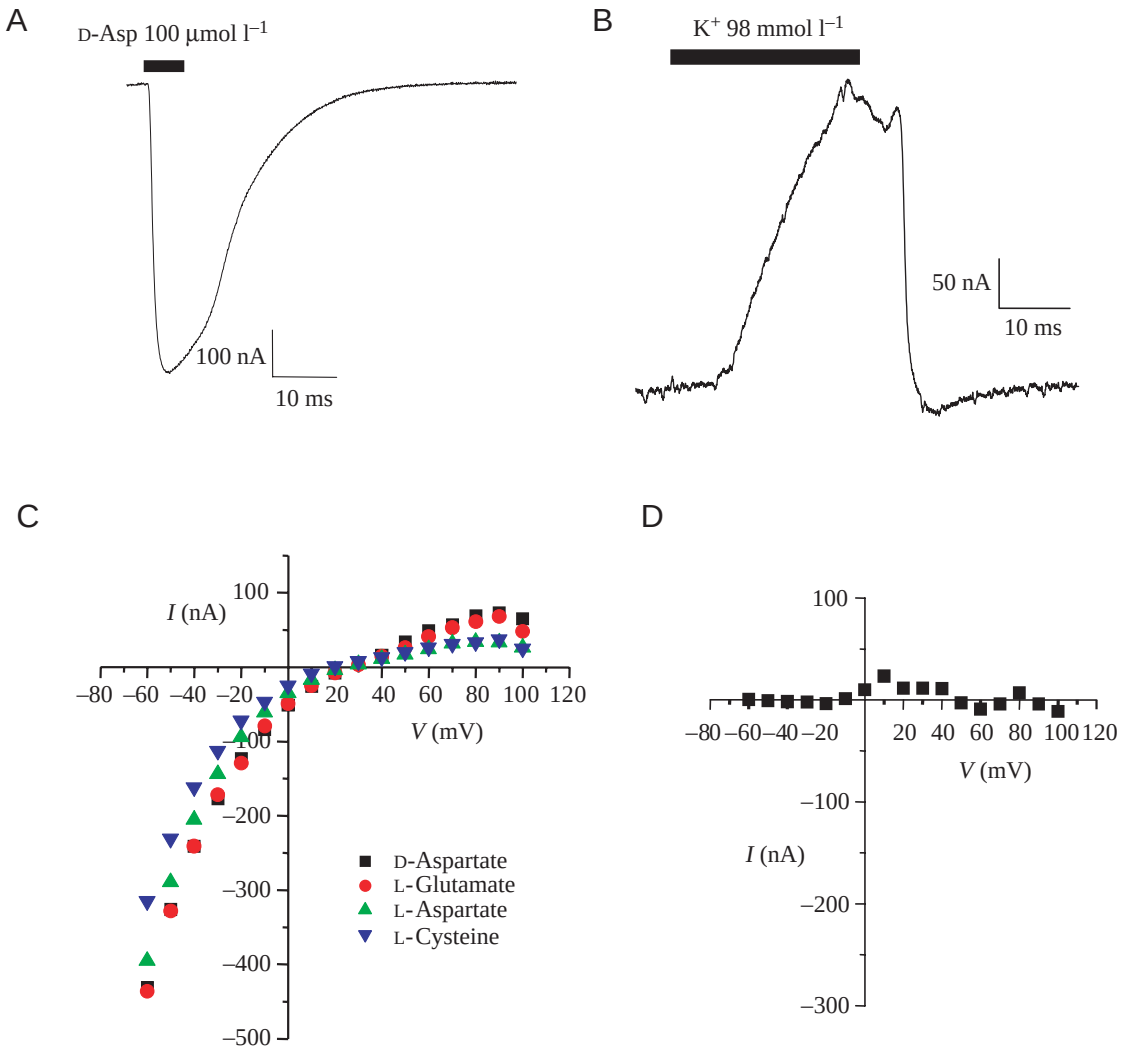

Fig. 5. Substrate-induced currents. (A) Inward currents induced by 100 µmol l^{-1} D-aspartate onto *Xenopus* oocytes expressing AeaEAAT for the duration indicated by the black bar. A holding potential of –60 mV was used. Similar inward currents were produced by application of L-Glu, L-Asp and L-Cys (data not shown). (B) Reversal of current upon exposing AeaEAAT-expressing oocytes to a sodium-free buffer containing a high potassium concentration (98 mmol l^{-1}), at a holding potential of –60 mV. This represents the transport of endogenous excitatory amino acids out of the oocyte, and was not observed in water-injected oocytes (data not shown). (C) AeaEAAT-mediated substrate-activated currents. These current–voltage relationships are the difference between substrate-activated currents and currents in the buffer alone, obtained by off-line subtraction of the steady state portion of voltage-jump curves. Reversal potentials for the four amino acids (L-Glu, L- and D-Asp and L-Cys) applied at 100 µmol l^{-1} each are approximately +37 mV. (D) Sodium dependence of substrate-activated currents. Replacement of extracellular sodium with equimolar choline completely abolishes the D-aspartate (100 µmol l^{-1})-activated current.

Expression in Xenopus laevis *oocytes*

In an attempt to understand the ion transport characteristics of AeaEAAT, we turned to heterologous expression of AeaEAAT in *Xenopus laevis* oocytes where two-electrode voltage clamp analysis was performed. *Xenopus* oocytes injected with cRNA *in vitro*-transcribed from pBSAMVBC10 displayed an inward current that is characteristic of this family of transporters upon application of substrate (Fig. 5A). This is consistent with a net inward flow of cations during the transport cycle (Zerangue and Kavanaugh, 1996b). Typically, the current elicited by the application of 100 µmol l^{-1} substrate was as large as 200–400 nA. Similar currents were produced regardless of the substrate (i.e. L-glutamate, L- and D-aspartate, L-cysteine).

Reversal of extracellular ionic composition by raising K^+ ion concentrations caused outward currents to be elicited by oocytes expressing AeaEAAT, reflecting the reversed transport of endogenous excitatory amino acids (Fig. 5B). No outward current was observed in water-injected oocytes upon exposure to high extracellular K^+ (data not shown). Endogenous excitatory amino acid concentration in *X. laevis* oocytes has been reported to be as high as 12 mmol l^{-1} (Wadiche et al., 1995a). Reversed transport is a physiologically relevant phenomenon in mammals that occurs in disease states such as

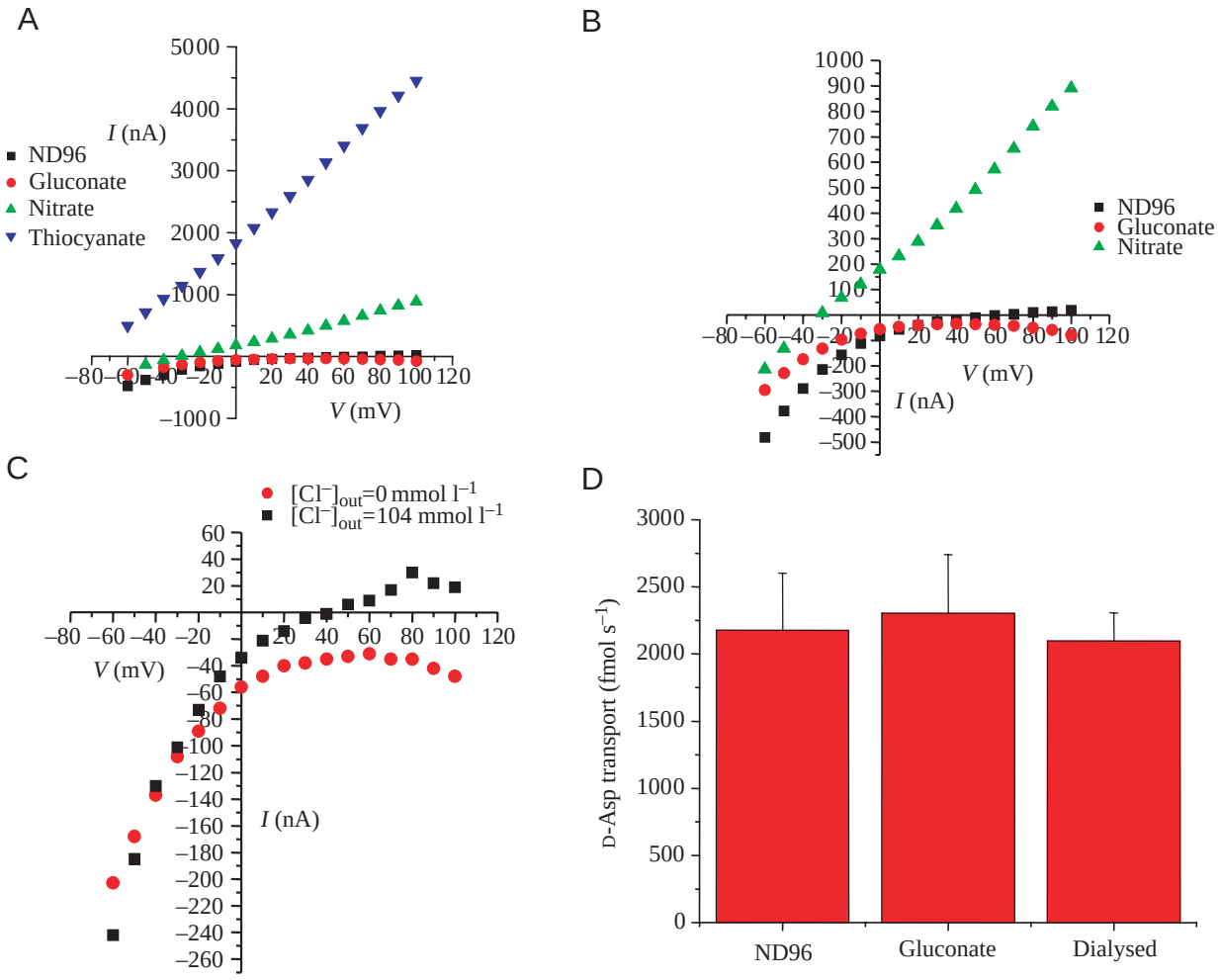

Fig. 6. Effect of Cl^- on substrate-induced transporter-mediated currents. (A) D-Aspartate (100 μmol l^{-1}) activated AeaEAAT currents in ND96 (squares) and various chloride-substituted buffers: gluconate (circles), nitrate (triangles) and thiocyanate (inverted triangles). (B) As A, but with currents in the thiocyanate buffer omitted, so as to expand the *y*-axis. (C) Substrate-induced current-voltage relationships upon dialysis of intracellular Cl^- from AeaEAAT-expressing oocytes, by incubation in Cl^--free saline substituted by gluconate at least 24 h prior to recordings. In the absence of intracellular Cl^-, the presence of extracellular Cl^- (squares) causes outward current. This outward current is absent when extracellular Cl^- is replaced by gluconate (circles). In all cases, currents were recorded from potentials between –60 and +50 mV in 10 mV intervals. (D) Radiolabeled ligand transport by oocytes under voltage clamp (–60 mV), in ND96 buffer, gluconate-substituted buffer (Gluconate), and dialysed oocytes in gluconate-substituted buffer (Dialysed).

ischemia, when extracellular concentrations of K^+ rise to 60 mmol l^{-1}, thereby depolarizing cells and allowing the release of glutamate by reversed functionality of the glutamate transporters (Attwell et al., 1993).

Difference *I–V* curves obtained by off-line subtraction of voltage-jump protocols without substrate from those with substrate, revealed a substrate-activated current reversing at 25–30 mV for all substrates tested (Fig. 5C). The substrate-activated current was abolished upon substitution of extracellular Na^+ with choline (Fig. 5D).

It is now well established that excitatory amino acid transporters carry a substrate-gated anion conductance that is not coupled to transport (reviewed in Seal and Amara, 1999). The ability of AeaEAAT to carry this type of current was determined by investigating the difference *I–V* curves upon replacement of extracellular Cl^- with other anions. Outward current was abolished when external chloride was replaced by gluconate (Fig. 6A,B), an impermeable anion, but enhanced when replaced with more permeant anions such as nitrate and thiocyanate (Fig. 6A,B). We then compared the substrate-activated currents of oocytes depleted of intracellular chloride by dialysis, in both the presence and absence of extracellular chloride (Fig. 6C). Chloride-dialysed oocytes gave identical inward currents regardless of the presence of extracellular chloride. However, outward currents were only seen in dialysed oocytes in the presence of extracellular Cl^-.

We addressed the question of whether substrate transport was dependent on the presence of either intracellular or extracellular Cl^-, by comparing radiolabeled substrate

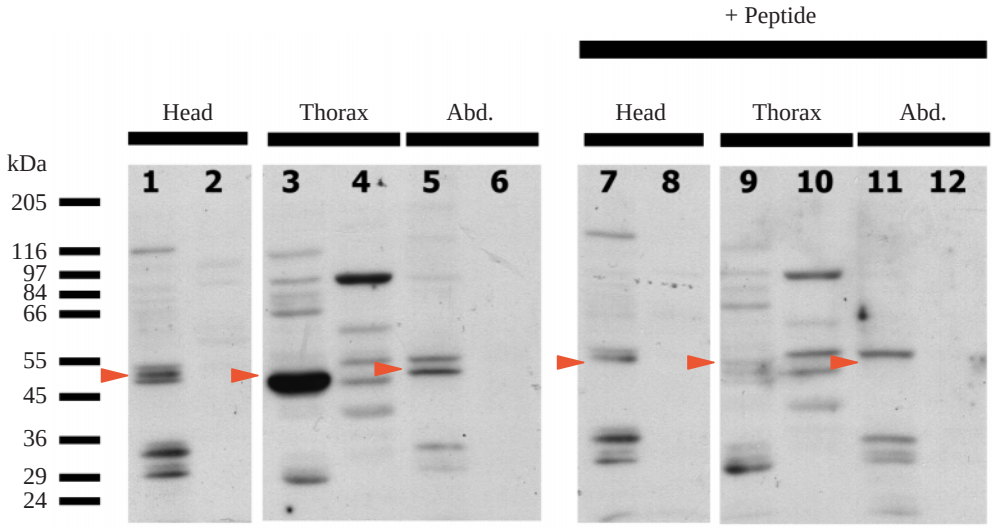

Fig. 7. Western analysis of adult *Ae. aegypti*. Membrane and cytosolic fractions separated from head (lanes 1, 2, 7, 8), thorax (lanes 3, 4, 9, 10) and abdomen (Abd., lanes 5, 6, 11, 12) of adult *Ae. aegypti* were probed with affinity-purified α-AeaEAAT antibody (lanes 1–6) or with the α-AeaEAAT antibody that had been preadsorbed with the antigenic peptide (10 μmol l^{-1}) (lanes 7–12). Odd-numbered lanes correspond to membrane fractions, and even-numbered lanes to cytosolic fractions. The α-AeaEAAT specific band migrates at a molecular mass of 50–52 kDa (arrowheads in lanes 1, 3, 5). Arrowheads in lanes 7, 9 and 11 indicate the missing band upon peptide preadsorption. The positions of molecular mass (kDa) proteins are shown.

transport of dialysed oocytes to undialysed oocytes while holding the membrane potential at –60 mV (Fig. 6D). Under these conditions, substrate transport was not compromised, in spite of a reduction in the transport associated current.

Western analysis

We addressed the question of AeaEAAT localization by generating a peptide antibody to a variable region of the protein. Affinity purification produced a specific antibody with high affinity for AeaEAAT, as characterized by ELISA (data not shown). When used in immunoblots against adult *Ae. aegypti* head membrane fractions (25 μg per lane), as well as membrane preparations of AeaEAAT expressing *Xenopus* oocytes (9 μg per lane), the antibody recognized a band at 52.5 kDa (Fig. 2, lanes 2 and 4). When membrane fractions isolated from the adult head, thorax, and abdomen regions were subjected to western analysis (25 μg per lane), a specific signal of 52.5 kDa was evident in all three regions (Fig. 7, lanes 1, 3, 5), with the most intense signal in the thorax (Fig. 7, lane 3). These bands could not be detected when peptide preadsorbed antibody was used to probe the blots (Fig. 7, lanes 7, 9, 11). Immunoreactive bands were absent in the cytosolic fractions (Fig. 7, lanes 2, 4, 6). The results shown in Fig. 7 are from adult males: identical results were obtained from adult females (data not shown).

Analogous experiments were conducted with larval and pupal membrane fractions to gather information on the developmental expression profile. Interestingly, only low levels of AeaEAAT immunoreactivity could be detected in larval head, thorax and abdomen membranes fractions even when 40 μg of protein was loaded per lane (data not shown). In the pupal stage, AeaEAAT immunoreactivity was negligible when 40 μg of membranes were probed (data not shown).

Immunohistochemistry

Based on the results from western analysis, we focused on the adult thorax for immunohistochemical studies. Paraffin sections of the adult thorax probed with the affinity-purified antibody revealed staining of neuropile regions of the thoracic ganglia (Fig. 8B,C). Immunoreactivity in this region was abolished when the antibody had been preadsorbed with the antigenic peptide (Fig. 8A). Staining of fibers in the neuropile region, as well as cell bodies peripheral to this region, could be observed (Fig. 8C, arrowheads). The muscles within the thorax, however, did not show immunoreactivity to this antibody.

Discussion

Here we have presented a comprehensive study on the cloning and functional characterization of a glutamate transporter isolated from a tissue-specific cDNA library from the midgut and Malpighian tubules of the adult female mosquito, *Aedes aegypti*, prior to blood feeding. We presented pharmacological and biophysical data on the heterologously expressed protein, and explored its tissue distribution using western analysis and immunohistochemistry.

At the amino acid level, AeaEAAT has greatest identity to its cloned insect counterparts, especially to DipEAAT, dEAAT1, and TrnEAAT. When compared to the five human homologues, AeaEAAT shares highest homology with the neuronal hEAAT3, whose rabbit homologue was originally

isolated from the kidney (Fig. 1B). For all cloned EAATs thus far, including AeaEAAT, sequence conservation is greatest at the C terminus, where 50–60% identity is observed. Hydropathy analysis gives proteins with intracellular N and C termini, having six clear transmembrane segments in the N terminus. The C-terminal transmembrane topology for this family of proteins has been a point of much debate, as despite the high degree of sequence conservation in this region, predictions based on hydrophobicity gave 0–4 transmembrane segments for different EAATs (Slotboom et al., 1999). More recent experimental studies of some mammalian counterparts suggest that the C-terminal half comprises a re-entrant loop structure with an outward-facing hydrophobic linker between the loop and final transmembrane domain (Grunewald et al., 1998; Seal and Amara, 1998; Seal et al., 2000).

In humans, apart from the high-affinity glutamate transporters (EAAT1-5), there are two Na^+-dependent neutral amino acid transporters with approximately 30% identity to EAAT1–5, possessing the 6-amino-acid signature sequence AAI/VFIAQ. The two proteins, ASCT1 and ASCT2, have the transport properties of system ASC, which transport alanine, serine, threonine and cysteine (Arriza et al., 1993; Shafqat et al., 1993; Utsunomiya-Tate et al., 1996). The five EAAT proteins and two ASCT proteins thus form a carrier superfamily. As with other EAATs, AeaEAAT shares lower identity (30–35%) with ASCT1 and ASCT2.

Analysis of the two completely sequenced insect genomes, namely *D. melanogaster* and *Anopheles gambiae*, show the presence of two and three EAAT homologues, respectively. The two in *D. melanogaster*, dEAAT1 and dEAAT2, have been cloned and shown to functionally transport glutamate and aspartate, while the three in *An. gambiae* (GenBank accession numbers: AAB01008807, AAB01008797 and AAB01008964) have yet to be cloned (Besson et al., 1999, 2000; Kosakai and Yoshino, 2001; Seal et al., 1998). Based on this information, it is likely that there are at least two genes in mosquitoes encoding glutamate/aspartate transporters. However, the lower identity of AeaEAAT (33.5%) with the third homologous EAAT sequence in *An. gambiae* (AAB01008964) resembles the level of identity observed with the mammalian System ASC transporters (approximately 30–35%), suggesting that it is a functional homologue of System ASC transporters rather than EAATs.

Based on the initial amino acid sequence analysis, as well

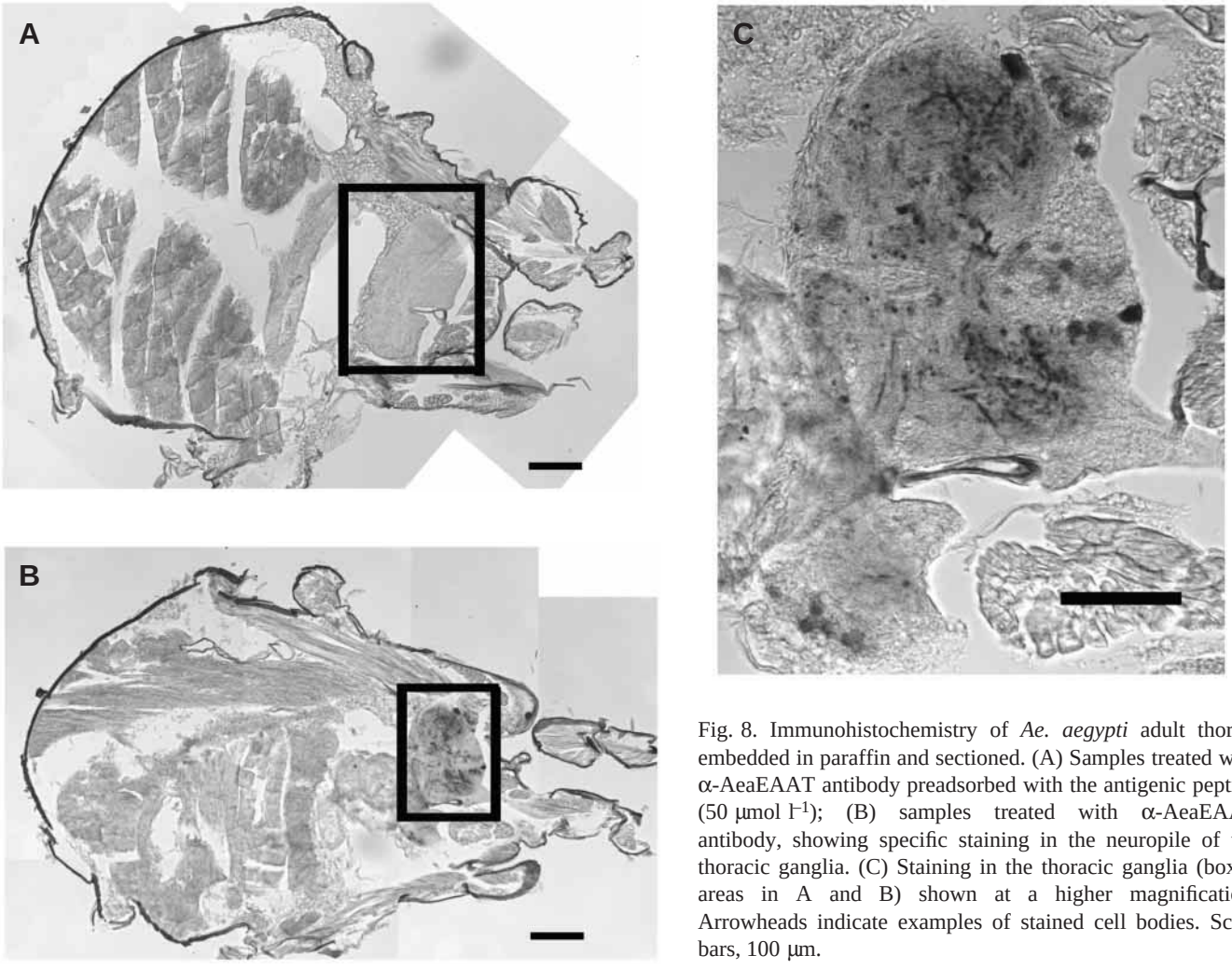

Fig. 8. Immunohistochemistry of *Ae. aegypti* adult thorax, embedded in paraffin and sectioned. (A) Samples treated with α-AeaEAAT antibody preadsorbed with the antigenic peptide (50 μmol l^{-1}); (B) samples treated with α-AeaEAAT antibody, showing specific staining in the neuropile of the thoracic ganglia. (C) Staining in the thoracic ganglia (boxed areas in A and B) shown at a higher magnification. Arrowheads indicate examples of stained cell bodies. Scale bars, 100 μm.

as the fact that AeaEAAT was originally isolated from a midgut/Malpighian tubule cDNA library, we heterologously expressed AeaEAAT in mammalian cells and *Xenopus* oocytes to test the hypothesis that it is the functional homologue of hEAAT3. Heterologously expressed AeaEAAT indeed transports glutamate and aspartate with high affinity (Table 1), sharing many of the properties seen with the mammalian EAATs, such as a strict dependence on extracellular Na^+ for function, and ability to perform reversed transport in the presence of high concentrations of extracellular K^+. A few lines of evidence prove our hypothesis that AeaEAAT is the functional homologue of hEAAT3. For example, analysis of AeaEAAT pharmacology excludes it from being the functional homologue of hEAAT2, as AeaEAAT is insensitive to DHK and KA, a property distinct to hEAAT2 (Table 2). With the exception of a unique sensitivity to serine-o-sulfate, pharmacological analysis of AeaEAAT using known blockers of glutamate transport shows its similarity to hEAAT1 and hEAAT3. Examination of substrate-elicited currents shows AeaEAAT to be responsive to L-cysteine (Fig. 5C), an amino acid which causes neuronal damage in mammals (Olney and Ho, 1970). Application of L-cysteine produces transporter-mediated currents specific for mammalian EAAT3, and thus additionally classifies AeaEAAT as an hEAAT3 orthologue (Zerangue and Kavanaugh, 1996c).

Profiles of difference *I–V* curves representing the substrate-activated transporter currents demonstrate AeaEAAT to be most similar to hEAAT3 as both reverse between +35 and +40 mV (Fig. 5C) (Wadiche et al., 1995a). Difference *I–V* curves for mammalian EAATs show clear reversal potentials ranging from +9 to +40 mV for hEAAT1–3, to –20 mV in the case of hEAAT4 and 5 (Arriza et al., 1997; Fairman et al., 1995; Wadiche et al., 1995a). Sodium-dependent solute transporters acting as secondary active carriers are not expected to reverse in polarity when exposed to extracellular substrate, regardless of the membrane potential, as seen for the rat GABA transporter (Mager et al., 1993). While reversals are not expected of classical secondary active carriers, they have been observed with transporters mediating substrate-evoked conductances that are not coupled to transport (Chaudhry et al., 2001; Fairman et al., 1995; Wadiche et al., 1995a). In particular, for mammalian EAATs the reversal has been attributed to a stoichiometrically uncoupled substrate-activated anion conductance, which is a property intrinsic to EAATs comprising (1) an anion leak in the absence of substrate, and (2) an anion channel-like activity evoked by the substrates of glutamate transport, but is not required for substrate transport (Arriza et al., 1997; Bergles and Jahr, 1997; Fairman et al., 1995; Otis and Jahr, 1998; Seal et al., 1998; Wadiche et al., 1995a; Wadiche and Kavanaugh, 1998). Although termed 'stoichiometrically uncoupled', this channel activity requires the presence of Na^+ and substrate, and is thought to be activated early in the transport cycle (Otis and Kavanaugh, 2000). The necessity for Na^+ and substrate is also apparent in our studies, since absence of both Na^+ and substrate evokes no transporter-mediated current (Fig. 5D).

While all five human EAATs exhibit a substrate-activated anion conductance, its contribution to the overall substrate-activated current differs. For example, more than 95% of the substrate-induced current is carried by Cl^- ions for hEAAT4 and hEAAT5 and 50–73% for hEAAT1-3 (Arriza et al., 1997). dEAAT1, the only other insect glutamate transporter studied by two-electrode voltage clamp, possesses a substrate-activated anion conductance that is responsible for most of the substrate-induced current. Furthermore, in the absence of intracellular and extracellular Cl^-, both substrate transport and substrate-induced currents by dEAAT1 are completely abolished (Seal et al., 1998).

Difference *I–V* curves upon anion substitution show AeaEAAT to elicit an analogous substrate-activated anion conductance, although the effect of Cl^- on AeaEAAT is not as dramatic as for dEAAT1 or hEAAT4 and 5. Replacement of extracellular Cl^- with gluconate, a more bulky anion, reduces the amplitude of both inward and outward currents, as for dEAAT1 (Fig. 6A,B), whereas substitution with more permeant anions such as NO_3^- and SCN^- increases the outward currents and shifts the reversal potential to values more negative than E_{Cl}, as seen for mammalian EAATs (Wadiche et al., 1995a; Zerangue and Kavanaugh, 1996a). The gluconate-mediated effects can be explained by employing explanations similar to those used for dEAAT1, where (1) the reduced outward current results from a reduction in inward anion permeation, and (2) the reduced inward current results from a reduced outward flow of Cl^- due to a change in the chemical gradient (Seal et al., 1998). On the other hand, effects of NO_3^- and SCN^- are due to increased permeation of these anions through AeaEAAT. Removal of both extracellular and intracellular Cl^- by dialysis with gluconate abolishes the reversal of the substrate-elicited current, while retaining an inward current (Fig. 6C), reflecting the coupled transport of substrate, Na^+, H^+ and countertransport of K^+. We conclude that the anion channel activity is not stoichiometrically coupled to substrate transport, since radiolabeled substrate transport under voltage clamp is not compromised regardless of the presence of Cl^- (Fig. 6D).

For the mammalian EAATs, the anion channel activity was recently separated from transport activity on a molecular level, where sulfhydryl modification of mutated residues V449C or V452C in hEAAT1 abolished substrate transport but not the anion conductance (Ryan and Vandenberg, 2002; Seal et al., 2001). These amino acids are conserved in AeaEAAT (V398 and V402) and could thus provide the basis for its ability to also exhibit an anion conductance. In summary, studies on the anion channel properties of AeaEAAT demonstrate its similarity to hEAAT1, 2 and 3, rather than hEAAT4 or hEAAT5. Coupled with the sequence comparisons and pharmacological studies discussed previously, these data strengthen the hypothesis that this protein is a functional homologue of hEAAT3.

Competition studies for D-aspartate transport by the 20 amino acids revealed statistically significant inhibition by L-glutamine and L-asparagine, amidated forms of the excitatory amino acid substrates (Fig. 4). While preliminary studies in our

laboratory implicate the ability of AeaEAAT to transport these amidated amino acids (data not shown), these results, as well as the L-glutamine and L-asparagine inhibition noted here, may be an artifact of trace contamination of L-glutamate and L-aspartate in the commercially available amino acids.

The final question addressed in this study is the localization of AeaEAAT, as it is still unclear whether insect EAATs participate in signal termination at invertebrate neuromuscular junctions. Only two recent reports have addressed this issue, where Soustelle et al. (2002) examined dEAAT1 and dEAAT2 expression *via in situ* hybridization, and Gardiner et al. (2002) studied TrnEAAT localization *via* immunohistochemistry. Results from both groups demonstrate the respective EAATs to be glial rather than neuronal. Gardiner et al. (2002) provided additional evidence for TrnEAAT localization in glia at both neuromuscular junctions and in neuropile regions of larval *T. ni*. The glial localization of these insect transporters illuminates the importance of glia in regulation of extracellular glutamate concentrations. Indeed, in humans it is believed that the glial transporters (hEAAT1 and hEAAT2) principally contribute to glutamate clearance in the brain, thereby preventing glutamate induced excitotoxicity. This has been demonstrated by EAAT knockout mice, in which mice lacking glial EAATs develop neurodegeneration and paralysis that are symptomatic of glutamate excitotoxicity (Rothstein et al., 1996; Tanaka et al., 1997).

Initial experiments to localize AeaEAAT by western analysis showed the greatest immunoreactivity in membrane fractions of the adult thorax (Fig. 8). Given the intensity of the immunoreactive band in thorax membranes compared with the head and abdomen membrane fractions, we initially hypothesized AeaEAAT to be present in adult thorax muscles, since the adult thorax is rich in muscles involved in flight and leg movement. However, immunohistochemistry results from the adult thorax showed specific staining in the neuropile regions of the thoracic ganglia but not in muscles (Fig. 8). The present data do not discriminate between the neuronal or glial localization of AeaEAAT, an issue which is currently being pursued. Nonetheless the results do suggest that AeaEAAT is not involved in termination of glutamatergic signals at the adult mosquito neuromuscular junction. Yet, based on the findings of Gardiner et al. (2002) that insect EAATs are indeed localized in muscles, as well as our hypothesis that a second functional EAAT exists in the mosquito genome (as discussed earlier), we postulate that the second mosquito EAAT would be responsible for termination of glutamatergic signals at the mosquito neuromuscular junction.

It is interesting to note that western analysis of analogous membrane fractions from fourth-instar larvae and day-2 pupae gave virtually negligible immunoreactivity, implying an increase of the AeaEAAT signal with development. Indeed, this is the case for dEAAT1, where the authors have noted that the onset of expression occurs in larval stages rather than in embryonic stages (Soustelle et al., 2002). Tissue-specific RT–PCR performed to localize AeaEAAT gave inconclusive results, as PCR products from genomic and cDNA gave identical sizes, indicating a lack of intronic sequences (data not shown).

In spite of the fact that this clone was originally isolated from an EST library of the adult female midgut/Malpighian tubule library, whole-mount immunolocalization studies using these tissues did not yield any positive results. We believe that this can be attributed to one of the following: (1) the present antibody is not capable of detecting AeaEAAT in the whole-mount preparations used, (2) the transcript, and therefore the protein is expressed below the limits of detection of immunocytochemical procedures, or (3) the clone was isolated from contaminating nerve or muscle tissue surrounding the midgut and Malpighian tubule tissues used to create the cDNA library.

The results presented in this study provide an insight to the role played by excitatory amino acid transporters in the mosquito, *Aedes aegypti*. Mosquitoes have historically been and still are the cause of many human diseases worldwide, including malaria, dengue, lymphtic filariasis, yellow fever, Japanese encephalitis and West Nile virus (Roberts, 2002). Together, there are over 500 million cases a year of mosquito-borne illnesses. Amidst the heightened interest in mosquito biology, the work presented is a timely contribution to the further understanding of this disease vector.

We thank Drs V. Filippov, Y. Park, C. S. Chiu, and M. E. Adams for valuable discussions throughout the course of this work; Dr Y. Zhao for expert technical guidance; Drs V. Filippov, M. L. Patrick and Ms H. R. Sanders for critically perusing the manuscript; and Ms A. Soderini-Coviella for maintaining the *Ae. aegypti* colony and help with dissections. This research was funded by grants AI 48049 to S.S.G. and a University of California Dissertation Research Grant to A.U.

References

Arriza, J. L., Eliasof, S., Kavanaugh, M. P. and Amara, S. G. (1997). Excitatory amino acid transporter 5, a retinal glutamate transporter coupled to a chloride conductance. *Proc. Natl. Acad. Sci. USA* **94**, 4155-4160.

Arriza, J. L., Kavanaugh, M. P., Fairman, W. A., Wu, Y. N., Murdoch, G. H., North, R. A. and Amara, S. G. (1993). Cloning and expression of a human neutral amino acid transporter with structural similarity to the glutamate transporter gene family. *J. Biol. Chem.* **268**, 15329-15332.

Attwell, D., Barbour, B. and Szatkowski, M. (1993). Nonvesicular release of neurotransmitter. *Neuron* **11**, 401-407.

Bergles, D. E. and Jahr, C. E. (1997). Synaptic activation of glutamate transporters in hippocampal astrocytes. *Neuron* **19**, 1297-1308.

Besson, M. T., Soustelle, L. and Birman, S. (1999). Identification and structural characterization of two genes encoding glutamate transporter homologues differently expressed in the nervous system of *Drosophila melanogaster*. *FEBS Lett.* **443**, 97-104.

Besson, M. T., Soustelle, L. and Birman, S. (2000). Selective high-affinity transport of aspartate by a *Drosophila* homologue of the excitatory amino-acid transporters. *Curr. Biol.* **10**, 207-210.

Blakely, R. D., Clark, J. A., Rudnick, G. and Amara, S. G. (1991). Vaccinia-T7 RNA polymerase expression system: evaluation for the expression cloning of plasma membrane transporters. *Anal. Biochem.* **194**, 302-308.

Buller, A. L. and White, M. M. (1992). Ligand-binding assays in *Xenopus* oocytes. In *Methods in Enzymology; Ion channels* (ed. B. Rudy and L. E. Iverson), pp. 368-375: San Diego, London: Academic Press, Inc.

Burrows, M. (1996). *The Neurobiology of an Insect Brain*. Oxford, New York: Oxford University Press.

Chaudhry, F. A., Krizaj, D., Larsson, P., Reimer, R. J., Wreden, C., Storm-Mathisen, J., Copenhagen, D., Kavanaugh, M. and Edwards, R. H. (2001). Coupled and uncoupled proton movement by amino acid transport system N. *EMBO J.* **20**, 7041-7051.

Cheng, Y. and Prusoff, W. H. (1973a). Relationship between the inhibition constant (K_i) and the concentration of inhibitor which causes 50 per cent inhibition (I_{50}) of an enzymatic reaction. *Biochem. Pharmacol.* **22**, 3099-3108.

Cheng, Y.-C. and Prusoff, W. H. (1973b). Relationship between the Inhibition Constant and the Concentration of Inhibitor Which Causes 50 Percent Inhibition of an Enzymatic Reaction. *Biochem. Pharmacol.* **22**, 3099-3108.

Chiu, C., Ross, L. S., Cohen, B. N., Lester, H. A. and Gill, S. S. (2000). The transporter-like protein inebriated mediates hyperosmotic stimuli through intracellular signaling. *J. Exp. Biol.* **203**, 3531-3546.

Cull-Candy, S. G. (1976). Two types of extrajunctional L-glutamate receptors in locust muscle fibres. *J. Physiol.* **255**, 449-464.

Danbolt, N. C. (2001). Glutamate uptake. *Prog. Neurobiol.* **65**, 1-105.

Darlison, M. G. (1992). Invertebrate GABA and glutamate receptors: molecular biology reveals predictable structures but some unusual pharmacologies. *Trends Neurosci.* **15**, 469-474.

Donly, B. C., Richman, A., Hawkins, E., McLean, H. and Caveney, S. (1997). Molecular cloning and functional expression of an insect high-affinity Na^+-dependent glutamate transporter. *Eur. J. Biochem.* **248**, 535-542.

Donly, C., Jevnikar, J., McLean, H. and Caveney, S. (2000). Substrate-stereoselectivity of a high-affinity glutamate transporter cloned from the CNS of the cockroach *Diploptera punctata*. *Insect Biochem. Mol. Biol.* **30**, 369-376.

Evans, P. D. (1975). The uptake of L-glutamate by the central nervous system of the cockroach, *Periplaneta americana*. *J. Exp. Biol.* **62**, 55-67.

Fairman, W. A., Vandenberg, R. J., Arriza, J. L., Kavanaugh, M. P. and Amara, S. G. (1995). An excitatory amino-acid transporter with properties of a ligand-gated chloride channel. *Nature* **375**, 599-603.

Gardiner, R. B., Ullensvang, K., Danbolt, N. C., Caveney, S. and Donly, B. C. (2002). Cellular distribution of a high-affinity glutamate transporter in the nervous system of the cabbage looper *Trichoplusia ni*. *J. Exp. Biol.* **205**, 2605-2613.

Grunewald, M., Bendahan, A. and Kanner, B. I. (1998). Biotinylation of single cysteine mutants of the glutamate transporter GLT-1 from rat brain reveals its unusual topology. *Neuron* **21**, 623-632.

Homberg, U. (1994). *Distribution of Neurotransmitters in the Insect Brain*. Stuttgart, New York: G. Fischer Verlag.

Kawano, T., Takuwa, K., Kuniyoshi, H., Juni, N., Nakajima, T., Yamamoto, D. and Kimura, Y. (1999). Cloning and characterization of a *Drosophila melanogaster* cDNA encoding a glutamate transporter. *Biosci. Biotechnol. Biochem.* **63**, 2042-2044.

Kerkut, G. A., Leake, L. D., Shapira, A., Cowan, S. and Walker, R. J. (1965). The presence of glutamate in nerve-muscle perfusates of Helix, Carcinus and Periplaneta. *Comp. Biochem. Physiol.* **15**, 485-502.

Kosakai, K. and Yoshino, M. (2001). A Na^+-dependent electrogenic glutamate transporter current in voltage-clamped cells of corpora allata in the cricket *Gryllus bimaculatus*. *J. Comp. Physiol. B* **171**, 303-312.

Kucharski, R., Ball, E. E., Hayward, D. C. and Maleszka, R. (2000). Molecular cloning and expression analysis of a cDNA encoding a glutamate transporter in the honeybee brain. *Gene* **242**, 399-405.

Laemmli, U. K. (1970). Cleavage of structural proteins during the assembly of the head of the bacteriophage T4. *Nature* **227**, 680-685.

Levy, L. M., Warr, O. and Attwell, D. (1998). Stoichiometry of the glial glutamate transporter GLT-1 expressed inducibly in a Chinese hamster ovary cell line selected for low endogenous Na^+-dependent glutamate uptake. *J. Neurosci.* **18**, 9620-9628.

Mager, S., Naeve, J., Quick, M., Labarca, C., Davidson, N. and Lester, H. A. (1993). Steady states, charge movements, and rates for a cloned GABA transporter expressed in *Xenopus* oocytes. *Neuron* **10**, 177-188.

Maragakis, N. J. and Rothstein, J. D. (2001). Glutamate transporters in neurologic disease. *Arch. Neurol.* **58**, 365-370.

Mbungu, D., Ross, L. S. and Gill, S. S. (1995). Cloning, functional expression, and pharmacology of a GABA transporter from *Manduca sexta*. *Arch. Biochem. Biophys.* **318**, 489-497.

Olney, J. W. and Ho, O. L. (1970). Brain damage in infant mice following oral intake of glutamate, aspartate or cysteine. *Nature* **227**, 609-611.

Otis, T. S. and Jahr, C. E. (1998). Anion currents and predicted glutamate flux through a neuronal glutamate transporter. *J. Neurosci.* **18**, 7099-7110.

Otis, T. S. and Kavanaugh, M. P. (2000). Isolation of current components and partial reaction cycles in the glial glutamate transporter EAAT2. *J. Neurosci.* **20**, 2749-2757.

Roberts, L. (2002). Mosquitoes and disease. *Science* **298**, 82-83.

Rothstein, J. D., Dykes-Hoberg, M., Pardo, C. A., Bristol, L. A., Jin, L., Kuncl, R. W., Kanai, Y., Hediger, M. A., Wang, Y., Schielke, J. P. et al. (1996). Knockout of glutamate transporters reveals a major role for astroglial transport in excitotoxicity and clearance of glutamate. *Neuron* **16**, 675-686.

Ryan, R. M. and Vandenberg, R. J. (2002). Distinct conformational states mediate the transport and anion channel properties of the glutamate transporter EAAT-1. *J. Biol. Chem.* **277**, 13494-13500.

Sattelle, D. B. (1992). Receptors for L-glutamate and GABA in the nervous system of an insect (*Periplaneta americana*). *Comp. Biochem. Physiol.* **103C**, 429-438.

Seal, R. P. and Amara, S. G. (1998). A reentrant loop domain in the glutamate carrier EAAT1 participates in substrate binding and translocation. *Neuron* **21**, 1487-1498.

Seal, R. P. and Amara, S. G. (1999). Excitatory amino acid transporters: a family in flux. *Annu. Rev. Pharmacol. Toxicol.* **39**, 431-456.

Seal, R. P., Daniels, G. M., Wolfgang, W. J., Forte, M. A. and Amara, S. G. (1998). Identification and characterization of a cDNA encoding a neuronal glutamate transporter from *Drosophila melanogaster*. *Recept. Chann.* **6**, 51-64.

Seal, R. P., Leighton, B. H. and Amara, S. G. (2000). A model for the topology of excitatory amino acid transporters determined by the extracellular accessibility of substituted cysteines. *Neuron* **25**, 695-706.

Seal, R. P., Shigeri, Y., Eliasof, S., Leighton, B. H. and Amara, S. G. (2001). Sulfhydryl modification of V449C in the glutamate transporter EAAT1 abolishes substrate transport but not the substrate-gated anion conductance. *Proc. Natl. Acad. Sci. USA* **98**, 15324-15329.

Shafqat, S., Tamarappoo, B. K., Kilberg, M. S., Puranam, R. S., McNamara, J. O., Guadano-Ferraz, A. and Fremeau, R. T., Jr (1993). Cloning and expression of a novel $Na(^+)$-dependent neutral amino acid transporter structurally related to mammalian Na^+/glutamate cotransporters. *J. Biol. Chem.* **268**, 15351-15355.

Slotboom, D. J., Konings, W. N. and Lolkema, J. S. (1999). Structural features of the glutamate transporter family. *Microbiol. Mol. Biol. Rev.* **63**, 293-307.

Soustelle, L., Besson, M. T., Rival, T. and Birman, S. (2002). Terminal glial differentiation involves regulated expression of the excitatory amino acid transporters in the *Drosophila* embryonic CNS. *Dev. Biol.* **248**, 294-306.

Tanaka, K., Watase, K., Manabe, T., Yamada, K., Watanabe, M., Takahashi, K., Iwama, H., Nishikawa, T., Ichihara, N., Kikuchi, T. et al. (1997). Epilepsy and exacerbation of brain injury in mice lacking the glutamate transporter GLT-1. *Science* **276**, 1699-1702.

Umesh, A. and Gill, S. S. (2002). Immunocytochemical localization of a *Manduca sexta* gamma-aminobutyric acid transporter. *J. Comp. Neurol.* **448**, 388-398.

Usherwood, P. N. (1967). Insect neuromuscular mechanisms. *Am. Zool.* **7**, 553-582.

Usherwood, P. N. and Machili, P. (1966). Chemical transmission at the insect excitatory neuromuscular synapse. *Nature* **210**, 634-636.

Utsunomiya-Tate, N., Endou, H. and Kanai, Y. (1996). Cloning and functional characterization of a system ASC-like Na^+-dependent neutral amino acid transporter. *J. Biol. Chem.* **271**, 14883-14890.

van Marle, J., Piek, T., Lind, A. and van Weeren-Kramer, J. (1983). Localization of a Na^+-dependent uptake system for glutamate in excitatory neuromuscular junctions of the locust *Schistocerca gregaria*. *Comp. Biochem. Physiol.* **74C**, 191-194.

Wadiche, J. I., Amara, S. G. and Kavanaugh, M. P. (1995a). Ion fluxes associated with excitatory amino acid transport. *Neuron* **15**, 721-728.

Wadiche, J. I., Arriza, J. L., Amara, S. G. and Kavanaugh, M. P. (1995b). Kinetics of a human glutamate transporter. *Neuron* **14**, 1019-1027.

Wadiche, J. I. and Kavanaugh, M. P. (1998). Macroscopic and microscopic properties of a cloned glutamate transporter/chloride channel. *J. Neurosci.* **18**, 7650-7661.

Zerangue, N. and Kavanaugh, M. P. (1996a). ASCT-1 is a neutral amino acid exchanger with chloride channel activity. *J. Biol. Chem.* **271**, 27991-27994.

Zerangue, N. and Kavanaugh, M. P. (1996b). Flux coupling in a neuronal glutamate transporter. *Nature* **383**, 634-637.

Zerangue, N. and Kavanaugh, M. P. (1996c). Interaction of L-cysteine with a human excitatory amino acid transporter. *J. Physiol.* **493**, 419-423.